18. Response latencies were given by the time of the first significant deviation of the derivative of the low-pass filtered (5-ms wide gaussian) averaged membrane potential waveform (t test, $P < 0.005$). The measure was validated when the peak of the rising waveform was significantly higher than that measured during the prestimulus trigger condition (t test, $P < 0.01$). Latency profiles were significantly (least-mean-square optimization) fitted by two straight lines (average $<r>^2 = 0.77$ with 2D impulse-like input and 0.88 with long bars), the intersection of which defined the retinal position of the latency basin center (Fig. 4, B and C). This center was superimposed on or close to the MDF center (relative eccentricity: 0.85 ± 0.7°).
19. Despite the fact that both the latency and the strength of the response were highly correlated with the relative eccentricity from the MDF center, both features of the postsynaptic response were weakly correlated together, thus reinforcing the hypothesis that the causative independent variable is the relative eccentricity itself.
20. Z. F. Kisvarday and U. T. Eysel, *Eur. J. Neurosci.* **5**, 1558 (1993).
21. A similar range of ASHP values is found in the adult cat if one takes into account the dependency of the cortical magnification factor on retinal eccentricity [K. Albus, *Exp. Brain Res.* **24**, 181 (1975); R. J. Tusa *et al.*, *J. Comp. Neurol.* **177**, 213 (1978)]. Furthermore, the ASHP values derived from individual latency basins are not significantly linked to the absolute retinal eccentricity of the discharge field of the recorded cells.
22. A. Grinvald *et al.*, *J. Neurosci.* **14**, 2545 (1994).
23. F. Chavane, V. Bringuier, Y. Frégnac, data not shown.
24. The typical speed of action potential propagation along horizontal excitatory connections is 0.15 to 0.60 m/s in T. Murakoshi *et al.* [*Neurosci. Lett.* **163**, 211 (1993)], 0.16 m/s in D. A. Nelson and L. C. Katz [*Neuron* **15**, 23 (1995)], and 0.35 m/s in J. A. Hirsch and C. D. Gilbert [*J. Neurosci.* **11**, 1800 (1991)]. A similar estimate is found for inhibitory connections: 0.06 to 0.20 m/s in P. Salin and D. A. Prince [*J. Neurophysiol.* **75**, 1589 (1996)].
25. The divergence of the terminal field of thalamocortical fibers extends over a 1- to 2-mm radius on average in the plane of cortical layers [A. L. Humphrey *et al.*, *J. Comp. Neurol.* **233**, 159 (1985)]. This value, replotted in visual field coordinates, is on the order of 1° to 2° of visual angle for central representation of the visual field and remains too low to explain the size of the D-field, which was found to be 4 to 15 times as large. Furthermore, the conduction velocity of X and Y thalamocortical axons is 10 to 100 times as fast as that derived from our measurements; the average ASHP value derived from our recordings is on the order of 0.15 m/s, whereas the conduction velocities of X and Y thalamic axons are, respectively, on the order of 8 and 20 m/s in H. P. Hoffmann and J. Stone [*Brain Res.* **32**, 460 (1971)].
26. A. C. Rosenquist, *Cereb. Cortex* **3**, 81 (1985).
27. Using identical stimuli, we obtained LGN ($n = 6$) and optic radiation ($n = 3$) discharge fields of restricted size (1.3° ± 0.6°). These controls preclude possible lateral excitation by light scatter in the retina.
28. A. Das and C. D. Gilbert, *Nature* **375**, 780 (1995).
29. We thank P. Godement, K. Grant, and P.-M. Lledo for helpful comments. We are indebted to L. Borg-Graham and C. Monier for patch electrode data, to D. E. Shulz and V. Ego for LGN recordings, and to P. Baudot, who participated in some of the experiments. This work was supported by CNRS, PROGRES-INSERM, AFIRST, GIS-Cognisciences, and Human Frontier Science Program (RG0103/1998-B) grants to Y.F.

28 July 1998; accepted 21 December 1998

Chemical Etiology of Nucleic Acid Structure: Comparing Pentopyranosyl-(2′→4′) Oligonucleotides with RNA

M. Beier, F. Reck, T. Wagner, R. Krishnamurthy, A. Eschenmoser*

All four members of the family of pentopyranosyl-(2′→4′) oligonucleotide systems that contain β-ribo-, β-xylo-, α-lyxo-, or α-arabinopyranosyl units as repeating sugar building blocks are found to be much stronger Watson-Crick base-pairing systems than RNA. The α-arabinopyranosyl system is the strongest of all and in fact belongs to the strongest oligonucleotide base-pairing systems known. Whatever the chemical determinants by which nature selected RNA as a genetic system, maximization of base-pairing strengths within the domain of pentose-derived oligonucleotide systems was not the critical selection criterion.

A chemical understanding of the criteria by which nature chose ribo- and deoxyribonucleic acids as genetic systems would constitute a central element of any theory of the origin of the particular kind of chemical life that we know today. The quest for such an understanding may be taken up by experiment by systematically synthesizing potential alternatives to the natural nucleic acids and comparing them with RNA with respect to those chemical properties that are fundamental to RNA's biological function (*1*). For such an alternative to be selected for study, we require it to be structurally derivable from a $(CH_2O)_n$ aldosugar ($n = 6$, 5, or 4) by the same type of potentially natural chemistry that allows the structure of RNA to be derived from ribose (*2*). This strategy is an attempt to mimic a hypothetical natural process that may have led to the selection of RNA: a process of combinatorial molecular assembly and functional selection within the domain of sugar-based oligonucleotides. In principle, such an experimental etiological analysis of nucleic acid structure is unbiased with respect to the question of whether RNA first came into being abiotically or biotically.

Our previous studies involving the β-hexopyranosyl-(4′→6′) oligonucleotide family had shown that base pairing in allo-, altro-, and glucopyranosyl oligonucleotides is uniformly much weaker than in RNA (*3*). Comparison with the properties of the 2′-deoxy, 3′-deoxy, and 2′,3′-dideoxyallopyranosyl analogs (*4*) demonstrated that the weaker base pairing is due to intrastrand steric hindrance in the pairing conformation ("too many atoms") (*3*). These findings led us to refocus our studies on the less bulky pentopyranosyl series, where it was discovered that the β-ribopyranosyl-(2′→4′) oligonucleotide system, the pyranosyl isomer of RNA (p-RNA), exhibits Watson-Crick pairing that is far stronger than that in RNA (*5*). Here we show that the same is true for the entire family of pentopyranosyl-(2′→4′) oligonucleotide systems that have the nucleotide base in the equatorial position of the pyranose chair (Scheme 1).

Scheme 2 summarizes the syntheses of the phosphoramidite building blocks **4**, **9**, and **13**, each prepared from the corresponding nucleosides containing adenine or thymine as the nucleobase (*6*, *7*). The preparation of oligomers in the lyxo- and xylopyranosyl series followed the (2′→4′) strategy previously applied in the p-RNA series (*5*). Inversely, oligomer synthesis in the α-arabinopyranosyl series was chosen to proceed in the (4′→2′) direction because the axial 4′-hydroxyl is the least reactive to electrophilic derivatization among the three hydroxyl groups (*8*).

Table 1 summarizes T_m values (the temperature at which about 50% of duplex molecules are dissociated into single strands) and thermodynamic data for five different octamer duplexes of each of the four pentopyranosyl-(2′→4′) oligonucleotide systems, determined in buffered 0.15 M sodium chloride solution at pH 7.0 (see also Fig. 1). Duplex formation was further characterized by temperature-dependent circular dichroism (CD) spectroscopy (Fig. 2) as well as by confirmation of strand stochiometry by determination of ultraviolet (UV) mixing curves

The Skaggs Institute for Chemical Biology at The Scripps Research Institute, 10550 North Torrey Pines Road, La Jolla, CA 92037, USA, and Laboratorium für Organische Chemie, Eidgenössische Technische Hochschule (ETH), Universitätstrasse 16, CH-8092 Zürich, Switzerland.

*To whom correspondence should be addressed.

for the $A_8 \cdot T_8$ duplexes. There is no self-pairing of single strands in the xylopyranosyl series, whereas in the more strongly pairing α-lyxopyranosyl system, both A_8 and T_8 exhibit weak self-pairing under high-salt conditions. In the arabinopyranosyl series, T_8 pairs weakly with itself, whereas A_8 does not (*9*).

All four members of the pentopyranosyl-(2′→4′) oligonucleotide family undergo markedly efficient cross-pairing with each other, at least with regard to duplex formation between A_8 and T_8 strands (*10*). Such a cross-pairing must reflect the capability of all members to adopt a common type of duplex structure. We view it as consisting of quasi-linear Watson-Crick paired double strands with antiparallel strand orientation and a left-handed helical twist, as previously postulated for the $(CGAATTCG)_2$ duplex in the ribopyranosyl series on the basis of nuclear magnetic resonance (NMR) structural analysis and molecular dynamics modeling (*5*). The structural similarity among the duplexes is also reflected in their common characteristics with respect to the sequence dependence of their stability. Sequence motifs of the form $(pyrimidine)_n$-$(purine)_n$ are more stable than those of the form $(purine)_n$-$(pyrimidine)_n$ in all four systems of the pentopyranosyl-(2′→4′) oligonucleotide family (Fig. 1). Such behavior was previously rationalized in the p-RNA series (*5*) as being the consequence of the overriding influence of interstrand base-stacking on duplex stability in oligonucleotide systems that show a strong inclination between backbone and base-pair axes. This interpretation is supported by the inverse sequence-motif dependence of duplex stability in the homo-DNA series where the sign of backbone–base pair inclination is opposite to that of p-RNA (*4*, *11*).

Base pairing in p-RNA had been shown to be Watson-Crick by NMR spectroscopy (*5*), and we conclude that the same holds for the entire pentopyranosyl family. Supporting this conclusion is the observation that the sequence dependence of duplex stabilities follows a similar pattern for each of the four pentopyranosyl systems (Fig. 1) (*12*). The CD spectra of β-xylo- and β-ribopyranosyl duplexes closely resemble each other, as do the spectra of α-lyxo- and α-arabinopyranosyl duplexes (Fig. 2).

The α-arabinopyranosyl system, as judged from its T_m values of adenine- and thymine-containing duplexes, belongs to the strongest phosphodiester-based oligonucleotide base-pairing systems encountered thus far (*13*). Its extraordinary pairing strength must be a consequence of the extensive steric constraint exerted on the phosphodiester group when flanked at the 2′-junction not only by the nucleobase, but also by the 3′-hydroxyl in an equatorial position (see arrows in Scheme 1); this constraint—in conjunction with the rigidity of the pyranose chair and the axial junction of the phosphodiester group at the 4′-carbon—may preorganize the single strand toward a pairing conformation (*4*). The phenomenon clearly calls for a detailed structural study (*14*). Because in the p-RNA series (*5*) the assessment of pairing behavior based on adenine-thymine pairing was found to be fully consistent with that derived from the behavior of guanine-cytosine–containing duplexes, we assume the same to be the case for all four pentopyranosyl-(2′→4′) oligonucleotide systems.

The finding that an entire family of potentially natural RNA isomers has a capability for Watson-Crick base pairing far more efficient than that of natural RNA itself needs to be put into an etiological perspective. From our present, although limited, knowledge of the range and type of chemistry that may have been involved in a primordial emergence of the RNA structure (*15*), we conjecture that such chemistry should have produced oligonucleotides derived not only from ribose, but from other aldopentoses as well, and that it might have led to both the furanosyl systems and the corresponding pyranosyl

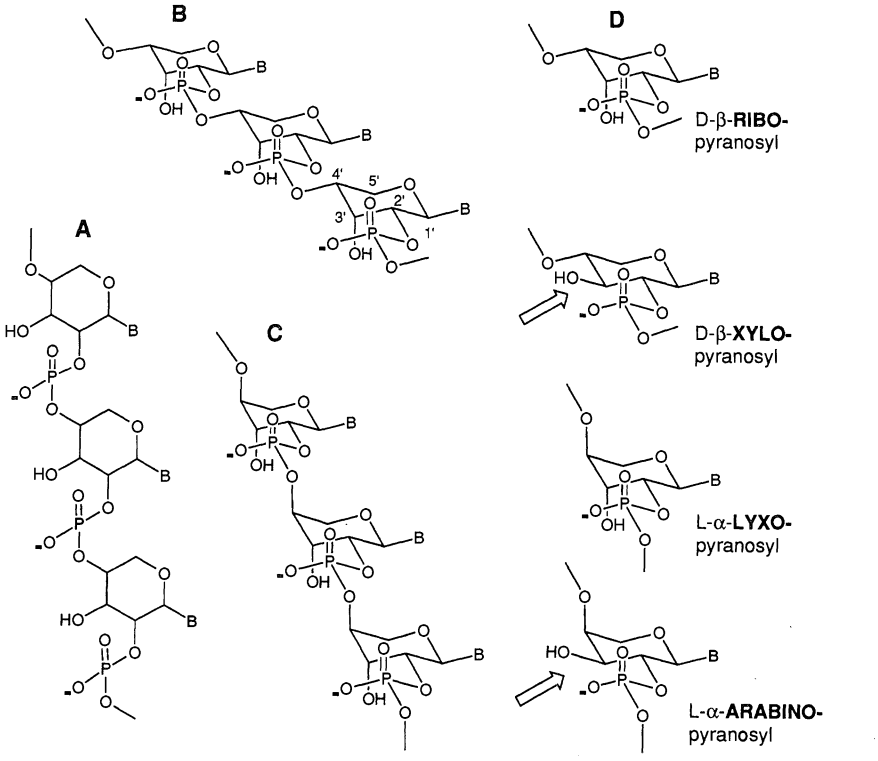

Scheme 1. (**A**) Constitution of the pentopyranosyl-(2′→4′) oligonucleotide family. B = nucleotide base. (**B**) Idealized pairing conformation in duplexes of (D)-β-ribopyranosyl-(2′→4′) oligonucleotides. (**C**) Idealized pairing conformation in duplexes of (L)-α-lyxopyranosyl-(2′→4′) oligonucleotides. (**D**) Configuration and (idealized) conformation of the repeating units of the four diastereomeric pentopyranosyl-(2′→4′) oligonucleotide systems discussed in this paper. Arrows (⇒) point to steric hindrance between equatorial hydroxyl and equatorial phosphate groups (equatorial substituents lie in averaged plane of pyranosyl chair, axial substituents perpendicular to it).

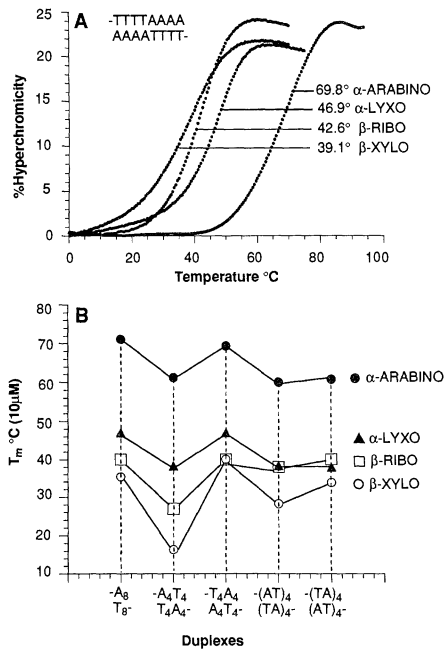

Fig. 1. (**A**) UV melting curves and T_m values of self-complementary strands T_4A_4 in the four pentopyranosyl-(2′→4′) oligonucleotide systems [strand concentration $c \sim 10$ μM, 0.15 M NaCl, 10 mM NaH_2PO_4, 0.1 mM Na_2EDTA (pH 7)]. (**B**) Thermal stabilities of octamer duplexes showing the pattern of sequence-motif dependence (for conditions see Table 1).

alternatives (*1*, *3*). In such a scenario, RNA eventually would have emerged from a library of structural alternatives by selection processes based on functional criteria. It is primarily with respect to this type of scenario that our findings are interpreted to demonstrate that whatever the decisive criterion responsible for nature's selection of RNA as a genetic system may have been, it was not the criterion of maximization of base-pairing strength. On the other hand, our observations substantiate the notion that it may have been optimization rather than maximization of the strength of base pairing that played a decisive role in RNA's emergence. Extension of the experimental approach to this question would call for an analysis of etiologically more demanding properties such as the capability of informational self-replication and the capacity to express a chemical phenotype (*16*). Preliminary information in this direction is available for p-RNA (*5*).

It is also conceivable that RNA entered the biological scene as a result of what would amount to a "frozen accident" in the sense that circumstances happened to favor a formation of the RNA structure in preference over alternatives. In that case, a synthetic rather than a functional selection would have been the primary determinant of RNA's emergence. Known chemical properties that could have facilitated such a synthetic selection include the intrinsic preference for ribose formation in kinetically (but not thermodynamically) controlled aldolizations (*17*), or the quenching of the furanose-pyranose equilibrium of ribose in favor of the furanose form by selective functionalization, for example, of the sterically most accessible 5-hydroxyl group (*18*). Much more experimental chemistry is required before an assessment of the chances of a synthetic selection of the RNA structure can be made, how-

Table 1. T_m values and thermodynamic data of duplex formation. T_m values refer to an overall oligomer concentration of 10 μM in 0.15 M NaCl, 0.01 M tris-HCl (pH 7.0) (values with asterisks indicate in 1.0 M NaCl); thermodynamic parameters were determined from plots of T_m^{-1} versus ln *c* [for method see (*20*)]; experimental error for Δ*H* was estimated to be ±5%. Data for β-ribopyranosyl duplexes are from Bolli *et al.* (*5*) and from (*11*). RNA data determined for comparison (with T instead of U) were provided by T. Vivlemore (ETH). For the automated synthesis, isolation, and characterization of pentopyranosyl-(2′→4′) oligonucleotides see (*5*) and (*7*).

Octamer Duplex	Pentopyranosyl oligonucleotide system		T_m (10 μM) °C in 0.15M NaCl		ΔG 25° C kcal/mol	ΔH kcal/mol	TΔS 25° C kcal/mol
4′ 2′ -AAAAAAAA TTTT TTTT- 2′ 4′	β-ribo		40	46.0*	-10.5	-62.2	-51.7
	α-lyxo		47.0	51.0*	-12.3	-69.5	-57.2
	β-xylo		35.4	47.3*	-8.2	-39.3	-31.1
	α-arabino		71.1	79.7*	-15.7	-60.6	-44.9
		RNA		16.3*	-7.3*	-33.7*	-26.4*
-AAAATTTT TTTTAAAA-	β-ribo		27		-7.3	-48.1	40.8
	α-lyxo		38.2		-9.4	-60.7	-51.3
	β-xylo		16.3		-6.1	-27.4	-21.3
	α-arabino		61.2		-13.5	-59.9	-46.4
		RNA		11.0*	-5.6*	-41.9*	-36.3*
-TTTTAAAA AAAATTTT-	β-ribo		40		-9.8	-59.9	-50.1
	α-lyxo		47.0		-11.4	-67.0	-53.6
	β-xylo		40.3		-8.7	-40.1	-31.4
	α-arabino		69.4		-14.5	-57.6	-43.0
		RNA		10.8*	-5.2*	-46.1*	-40.9*
-ATATATAT TATATATA-	β-ribo		38		-9.2	-58.7	-49.5
	α-lyxo		38.3		-9.5	-61.4	-52.0
	β-xylo		28.6		-6.2	-33.9	-26.7
	α-arabino		60.0		---	---	---
-TATATATA ATATATAT-	β-ribo		40		-9.3	-51.6	-42.3
	α-lyxo		37.9		-9.4	-62.9	-53.5
	β-xylo		33.8		-7.6	-28.7	-21.1
	α-arabino		60.8		---	---	---

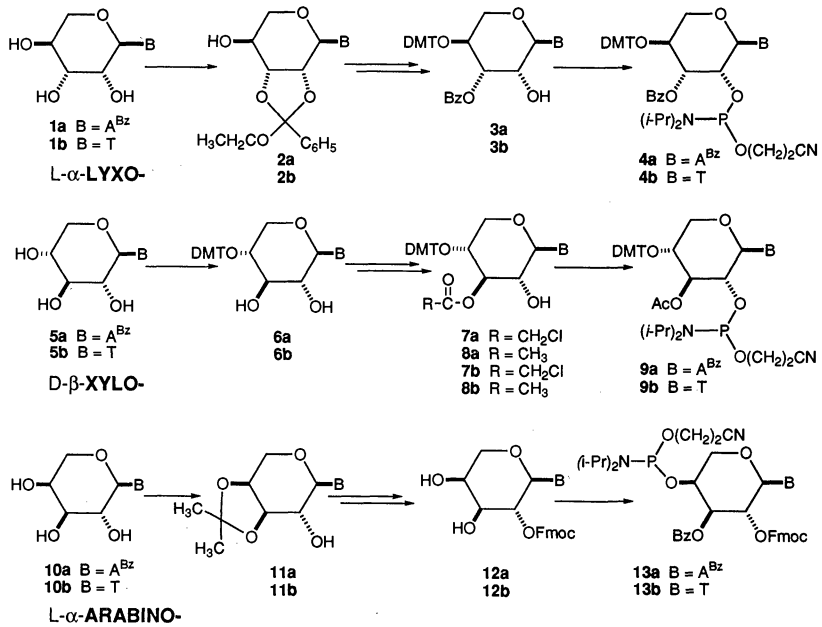

Scheme 2. F_{moc} = 9-fluorenylmethoxycarbonyl; A^{Bz} = 6-benzoylamino-purine-9-yl; T = thymine-1-yl; numbers before reagents denote mole equivalents, % denotes yield. Preparation of building blocks for oligonucleotide synthesis (*7*). (L)-α-Lyxopyranosyl series: **1a** (**1b**)→**2a** (**2b**): 2.0 (2.5) triethylorthobenzoate, 0.9 (0.3) p-TsOH, DMF/CH_3CN, 30°C, 2 hours, 64% (74%); **2a** (**2b**)→**3a** (**3b**): (a) 3.0 DMTrCl, 6 lutidine, CH_2Cl_2, 0°C, 8 hours; (b) 80 pct. CH_3CO_2H/THF/CH_2Cl_2 1:2:2, 23°C, 55% (61%); **3a** (**3b**)→**4a** (**4b**): 2.5 P((i-Pr)$_2$N)(OCH$_2$CH$_2$CN)Cl, 7.5 collidine, 0.5 N methylimidazole, CH_2Cl_2, 23°C, 10 min, 85% (80%). (D)-β-Xylopyranosyl series: **5a** (**5b**)→**6a** (**6b**): 2.5 DMTrCl, pyridine, room temperature (RT), 12 hours, 38% (34%) after chromatographic separation from isomers; **6a** (**6b**)→**7a** (**7b**): 1.5 chloroacetic acid anhydride, CH_2Cl_2/pyridine 4:1, 0°C, 1 hour, 45% (43%) after chromatography; **7a** (**7b**)→**8a** (**8b**): H_2/10 pct. Pd(C), THF, 3.0 K_2CO_3, 96% (91%); **8a** (**8b**)→**9a** (**9b**): 3.0 P((*i*-Pr)$_2$N)(OCH$_2$CH$_2$CN)Cl, 4.0 ethyldiisopropylamine, CH_2Cl_2, 23°C, 3 hours, 62% (81%). (D)-α-Arabinopyranosyl series: **10a**→**11a**: 3.0 2-methoxypropene, 0.03 TsOH, DMF, 0°C, 36 hours, 87%; **10b**→**11b**: 1.0 **10b** as Na salt, DMF, 1.2 HCl in dioxane, 1.7 2-methoxypropene, RT, 1.5 hours, 85%; **11a** (**11b**)→**12a** (**12b**): (a) 1.0 F_{moc}Cl, pyridine/CH_2Cl_2 3:1, 0°C→RT, 21 hours (1.5 hours), 87% (76%) of acetal derivative; (b) 80 pct. aqueous CH_3CO_2H, RT, 48 hours, 72% (0.026 M HCl in CH_3OH, 50°C, 2 hours, 74%). **12a** (**12b**)→**13a** (**13b**): (a) 1.8 (1.2) BzCl, 4.8 (3.5) pyridine, CH_2Cl_2/THF 5:1 (CH_2Cl_2), 0°C→RT, 16 hours (3.5 hours), 69% (85%) of 3′-benzoyl derivative; (b) 2.5 P((*i*-Pr)$_2$N)(OCH$_2$CH$_2$CN)Cl, 0.5 imidazole, 4.0 *N*-methylmorpholine (0.5 collidine), THF, 1 hour, RT, 62% (60%). Solvents were dried by treatment with 4 Å molecular sieves. Experiments starting from arabinose have been carried out in the (D) series, which is enantiomeric to the series depicted in Schemes 1 and 2.

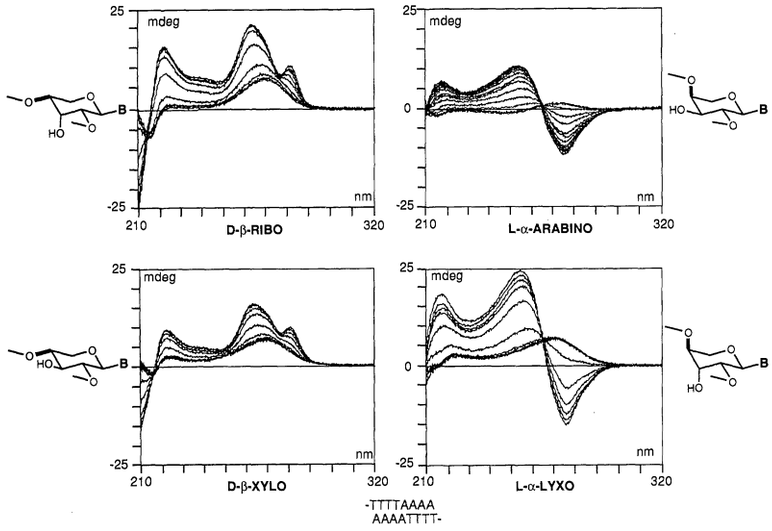

Fig. 2. Temperature-dependent CD spectra of the self-complementary sequences T_4A_4 in the four diastereomeric pentopyranosyl-(2′→4′) oligonucleotide systems [$c \approx 10$ μM, 0.15 M NaCl, 10 mM NaH_2PO_4, 0.1 mM Na_2EDTA (pH 7.0)]. T_m values derived from these CD curves: 41.1°C (β-ribo), 39.2°C (β-xylo), 45.4°C (α-lyxo), 66.1°C (α-arabino). CD spectrum of α-arabinopyranosyl duplex has been measured with a sample of the (D) series and is reproduced here as its mirror image.

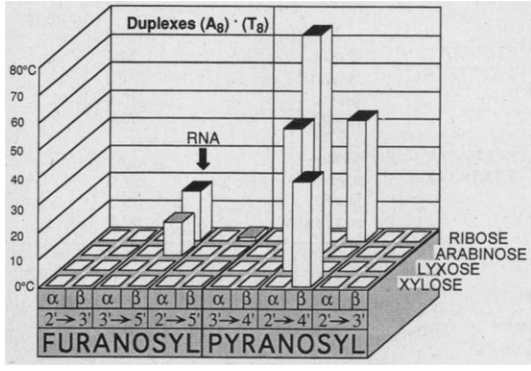

Fig. 3. Base-pairing–strength landscape of pentofuranosyl- and pentopyranosyl oligonucleotide systems showing the range of the constitutional and configurational diversity of (potentially natural) alternatives of the RNA structure and giving the T_m values of A_8·T_8 duplexes of the systems investigated so far (5+5 μM, 1.0 M NaCl). Black top of columns: T_m measured; shaded top of columns: T_m estimated; empty squares: not investigated. The value for the β-arabinofuranosyl-(3′→5′) system is estimated from data provided by W. Pfleiderer (*21*), that of the ribofuranosyl-(2′→5′) system from data reported in (*2*). For the other T_m values see Table 1.

ever. Finally, there is the possibility that RNA emerged within, or through the mediation of, an evolving biological system that later became extinct (*15*, *19*). In such a case, the determinant for RNA's selection could have been synthetic, functional, or both. Our conclusion regarding the role of pairing strength as a selection criterion for RNA remains valid independently of the actual determinant of RNA's selection.

The pairing-strength landscape shown in Fig. 3, in which natural RNA appears as a minor player, calls for charting other parts of the structural neighborhood of RNA with regard to its base-pairing potential. Within the pentopyranosyl domain, the members studied thus far are those that form preferentially under conditions of a conventional nucleosidation reaction and, therefore, may be of primary interest in an etiological context. However, the variants with inverted configuration at the anomeric center, or systems with phosphodiester junctions between positions other than 2′ and 4′, also deserve to be studied. An experimentally explored pairing-strength landscape of isomeric oligonucleotide systems would represent an exceptional source of reference data for a comprehensive analysis of the conformational and constellational factors that determine base pairing in nucleic acids. Our present data also may encourage attempts to map the complete pairing-strength landscape of RNA's structural neighborhood by theoretical methods.

References and Notes

1. A. Eschenmoser, in *Verh. Ges. Dtsch. Naturforsch. Aerzte* **116**, 135 (1990); _____ and M. Dobler, *Helv. Chim. Acta* **75**, 218 (1992); A. Eschenmoser and E. Loewenthal, *Chem. Soc. Rev.* **21**, 1 (1992); A. Eschenmoser, in *Proc. Robert A. Welch Found. Conf. Chem. Res. 37* (Robert A. Welch Foundation, Houston, TX, 1993), p. 201.
2. The closest structural alternative to RNA that satisfies this criterion is the RNA isomer containing (2′→5′)- instead of the (3′→5′)-phosphodiester junctions. For studies on this system in the etiological context, see L. E. Orgel, *J. Mol. Biol.* **38**, 381 (1968); _____ and R. Lohrmann, *Acc. Chem. Res.* **7**, 368 (1974); D. A. Usher, *Nature New Biol.* **235**, 207 (1972); _____ and A. H. McHale, *Proc. Natl. Acad. Sci. U.S.A.* **73**, 1149 (1976); R. Kierzek, L. He, D. H. Turner, *Nucleic Acids Res.* **20**, 1685 (1992); T. P. Prakash, C. Roberts, C. Switzer, *Angew. Chem. Int. Ed. Engl.* **36**, 1522 (1997); H. Sawai, J. Seki, H. Ozaki, *J. Biomol. Struct. Dyn.* **13**, 1043 (1996). For studies on the related (2′→5′) DNA isomer, see J. P. Dougherty, C. J. Rizzo, R. Breslow, *J. Am. Chem. Soc.* **114**, 6254 (1992); H. Hashimoto and C. Switzer, *ibid.*, p. 6255; T. P. Prakash, K.-E. Jung, C. Switzer, *Chem. Commun.* 1793 (1996).
3. A. Eschenmoser, *Origins Life Evol. Biosphere* **24**, 389 (1994).
4. J. Hunziker *et al.*, *Helv. Chim. Acta* **76**, 259 (1993); G. Otting *et al.*, *ibid.*, p. 2701; K. Groebke *et al.*, *ibid.* **81**, 375 (1998).
5. S. Pitsch, S. Wendeborn, B. Jaun, A. Eschenmoser, *ibid.* **76**, 2161 (1993) (synthesis and pairing properties); S. Pitsch *et al.*, *ibid.* **78**, 1621 (1995) (pairing properties); I. Schlönvogt *et al.*, *ibid.* **79**, 2316 (1996) (NMR structure); R. Krishnamurthy *et al.*, *Angew. Chem. Int. Ed. Engl.* **35**, 1537 (1996) (enantio pairing); R. Micura, M. Bolli, N. Windhab, A. Eschenmoser, *ibid.* **36**, 870 (1997) (hairpin formation); M. Bolli, R. Micura, S. Pitsch, A. Eschenmoser, *Helv. Chim. Acta* **80**, 1901 (1997) (replication); M. Bolli, R. Micura, A. Eschenmoser, *Chem. Biol.* **4**, 309 (1997) (self-templated oligomerization).
6. For pentopyranosyl-mononucleosides prepared for biological testing, see M. Fuertes, J. T. Witkowski, R. K. Robins, *J. Org. Chem.* **40**, 2372 (1975); A. P. Martinez, W. W. Lee, L. Goodman, *ibid.* **34**, 92 (1969); A. P. Martinez and W. W. Lee, *ibid.*, p. 416; _____, L. Goodman, *J. Med. Chem.* **12**, 1125 (1969). See also B. Doboszewski, N. Blaton, J. Rozenski, A. De Bruyn, P. Herdewijn, *Tetrahedron* **51**, 5381 (1995).
7. (L)-α-Lyxopyranosyl series: Orthoester formation involving the *cis*-2′,3′-diol function serves as transient protection of hydroxyl groups during 4′-tritylation and, at the same time, as a first step toward 3′-benzoylation; for selective formation of axial benzoates from cyclic orthobenzoates in pyranosides see R. U. Lemieux and H. Driguez, *J. Am. Chem. Soc.* **97**, 4069 (1975); S. Oscarson and A.-K. Tidén, *Carbohydr. Res.* **247**, 323 (1993). (D)-β-Xylopyranosyl series: Acylations of **6a/b** in pyridine produce preferentially the 2′-acyl derivatives which, however, slowly rearrange to the more stable 3′-acyl derivatives; chloroacetyl rearranges much faster than acetyl. (D)-α-Arabinopyranosyl series: For protection of the 2′-hydroxyl, a group that is inert to acids (F_{moc}) was chosen because, for its selective introduction, transient protection of the *cis*-3′,4′-diol function as an acetal was used. Oligomer synthesis proceeds in the (4′→2′) direction, with benzoyl as the protection group for the 3′-hydroxyl in conjunction with the linker system LCAMA-CPG [K.-P. Stengele and W. Pfleiderer, *Nucleic Acids Res. Symp. Ser.* **21**, 101 (1989)], which is stable to the conditions of base-induced eliminative deprotection involving the F_{moc} group.
8. Details concerning preparation of building blocks and automated syntheses of oligomers in the three new pentopyranosyl-(2′→4′) oligonucleotide series will be published in *Helv. Chim. Acta* [F. Reck, H. Wippo, R. Kudick (L-α-lyxopyranosyl series); M. Beier and O. Jungmann (D- and L-α-arabinopyranosyl series); T. Wagner (D-β-xylopyranosyl series); R. Krishnamurthy and A. Eschenmoser, in preparation].
9. T_m values of self-pairings (10 μM): pl(A_8) 15°C and pl(T_8) <5°C in 1.0 M NaCl; pa(T_8) 17°C in 0.15 M NaCl and 28°C in 1.0 M NaCl; UV and CD of pa(A_8) are essentially unchanged in the range 10° to 80°C (1.0 M NaCl).
10. T_m values of cross-pairing (5 μM each strand, in 1.0 M NaCl): pl(A_8)/pr(T_8) 31°C; pl(T_8)/pr(A_8) 43°C; pa(T_8)/pr(D_8) 55°C; px(A_8)/pr(T_8) 46°C; px(T_8)/pr(A_8) 45°C; pl(A_8)/px(T_8) 27°C; pl(T_8)/px(A_8) 42°C. Cross-pairing experiments involving the (D)-pa sequences have been carried out with (L)-pr sequences. No cross-pairing was observed between A_8 or T_8

strands of the (D)-pr-, (L)-pl-, and (D)-px series with complementary strands of the (D)-r series. For (L)-pr sequences, see (5). β-pr = ribo-, α-pl = lyxo-, β-px = xylo-, and α-pa = arabinopyranosyl; D = 2,6-diaminopurine.
11. R. Micura, R. Kudick, S. Pitsch, A. Eschenmoser, *Angew. Chem.*, in press; see also M. Bolli *et al.* (5).
12. For such relative duplex stabilities when base pairing is not Watson-Crick but Hoogsteen, see M. Bolli, J. C. Litten, R. Schütz, C. J. Leumann, *Chem. Biol.* **3**, 197 (1996).
13. For recently described strong base-pairing systems of the phosphodiester type, compare with R. Steffens and C. J. Leumann, *J. Am. Chem. Soc.* **119**, 11548 (1997); S. K. Singh, P. Nielsen, A. A. Koshkin, J. Wengel, *Chem. Commun.*, 455 (1998).
14. An NMR structure analysis of the α-arabinopyranosyl heptamer duplex $[pa(ATATATA)]_2$ (T_m = 57°C, 10 μM, 0.15 M NaCl) is being carried out in the laboratory of B. Jaun (ETH).
15. G. F. Joyce and L. E. Orgel, in *The RNA World*, R. F. Gesteland and J. F. Atkins, Eds. (Cold Spring Harbor Laboratory Press, Cold Spring Harbor, NY, 1993), p. 1.
16. A chemical phenotype of an informational system involves the whole of sequence-specific (and thus "inheritable") reactivities and catalytic properties apt to act as selection factors in the system's replication. Compare with A. Eschenmoser, *Origins Life Evol. Biosphere* **27**, 535 (1997).
17. D. Müller *et al.*, *Helv. Chim. Acta.* **73**, 1410 (1990); G. Zubay, *Origins Life Evol. Biosphere* **28**, 13 (1998); R. Krishnamurthy, S. Pitsch, G. Arrhenius, *ibid.*, in press.
18. B. Bennua-Skalmowski, K. Krolikiewicz, H. Vorbrüggen, *Tetrahedron Lett.* **36**, 7845 (1995); J. Wengel and C. Scheuer-Larsen, *Bioorg. Med. Chem. Lett.* **7**, 1999 (1997).
19. A. G. Cairns-Smith, *Genetic Takeover and the Mineral Origin of Life* (Cambridge Univ. Press, Cambridge, 1982); G. F. Joyce, A. W. Schwartz, S. L. Miller, L. E. Orgel, *Proc. Natl. Acad. Sci. U.S.A.* **84**, 4398 (1987).
20. L. A. Marky and K. J. Breslauer, *Biopolymers* **26**, 1601 (1987).
21. M. Resmini, thesis, Universität Konstanz, Germany, 1993 (W. Pfleiderer).
22. Supported by The Skaggs Research Foundation. M.B. and T.W. thank the Deutsche Forschungsgemeinschaft for fellowship support. We thank W. Pfleiderer (Universität Konstanz) for providing sequences of β-arabinofuranosyl-(3′→5′) oligonucleotides for T_m determinations, and G. Joyce (La Jolla) for critically reading the manuscript.

8 October 1998; accepted 29 December 1998

Reduced Immunotoxicity and Preservation of Antibacterial Activity in a Releasable Side-Chain Carbapenem Antibiotic

Hugh Rosen,* Richard Hajdu, Lynn Silver, Helmut Kropp, Karen Dorso, Joyce Kohler, Jon G. Sundelof, Joann Huber, Gail G. Hammond, Jesse J. Jackson, Charles J. Gill, Randall Thompson, Barbara A. Pelak, Jeffrey H. Epstein-Toney, George Lankas, Robert R. Wilkening, Kenneth J. Wildonger, Timothy A. Blizzard, Frank P. DiNinno, Ronald W. Ratcliffe, James V. Heck, John W. Kozarich, Milton L. Hammond

A carbapenem antibiotic, L-786,392, was designed so that the side chain that provides high-affinity binding to the penicillin-binding proteins responsible for bacterial resistance was also the structural basis for ameliorating immunopathology. Expulsion of the side chain upon opening of the beta-lactam ring retained antibacterial activity while safely expelling the immunodominant epitope. L-786,392 was well tolerated in animal safety studies and had significant in vitro and in vivo activities against methicillin- and vancomycin-resistant Staphylococci and vancomycin-resistant Enterococci.

The increasing prevalence of resistance in Staphylococci and Enterococci to currently available antimicrobials has resulted in the significant diminution of therapeutic options available. Patients infected with multi–drug resistant organisms are once again succumbing to sepsis (*1*). One approach to counter this is to directly target the molecular mechanism of resistance in an existing class of antimicrobials, restoring their effectiveness. Methicillin resistance in Staphylococci is generally dependent on the production of a unique penicillin-binding protein (PBP), PBP2a, which like other high molecular weight PBPs, catalyzes the transpeptidation of peptidoglycan. PBP2a has a relatively low affinity to all the common β-lactam antibiotics and, in the presence of antibiotic, is able to take on the critical tasks of cell wall remodeling normally performed by the more antibiotic-susceptible PBPs (*2*).

Carbapenems acylate a broad spectrum of PBPs with high affinity. They are rapidly bactericidal, with potent activity against methicillin-sensitive staphylococci. These intrinsic properties, together with multiple PBP targets, result in low frequency of resistance selection. In addition, the carbapenem nucleus is resistant to most serine β-lactamases, whether of staphylococcal, enterococcal, or Gram-negative origin (*3*). We previously described a series of carbapenems with improved affinities for PBP2a, and concomitant activity against methicillin-resistant *Staphylococcus aureus* (MRSA) (*4*). Improved affinity for PBP2a was related to the presence of a large lipophilic substituent attached to the carbapenem nucleus. Unfortunately, carbapenems optimized for their PBP2a affinity provoked immune responses in rhesus monkeys (*5*), including high-frequency immune-mediated hemolytic anemia with Coombs positivity, a peripheral blood lymphocytosis, and diffuse lymphoid hyperplasia of spleen and lymph nodes at subhemolytic doses (15 mg/kg body weight/day of L-742,728). These nonanaphylactic autoimmune syndromes are occasionally observed with lower frequency and at higher doses in response to β-lactams in clinical use (*6*).

Sera from rhesus macaques exposed to the carbapenems L-742,728, L-741,462, and L-695,256 (*7*) all showed high titer, drug-specific antibodies that could be affinity purified on drug-sepharose columns and agglu-

Table 1. Comparative in vitro antibacterial activity of L-786,392, imipenem, and vancomycin on Staphylococci and Enterococci.

Organism (number of strains)	MIC_{90} (μg/ml)		
	L-786,392	Vancomycin	Imipenem
Methicillin-susceptible *S. aureus* (15)	0.06	2	0.03
Methicillin-resistant *S. aureus* (42)	4	2	256
Methicillin-susceptible coagulase-negative *Staphylococcus* spp. (23)	0.016	2	0.03
Methicillin-resistant coagulase-negative *Staphylococcus* spp. (25)	4	4	256
Vancomycin-susceptible *E. faecalis* (17)	1	2	1
Vancomycin-resistant *E. faecalis* (15)	4	1024	2
Vancomycin-susceptible *E. faecium* (12)	2	2	64
Vancomycin-resistant *E. faecium* (31)	8	2048	>128
Enterococcus gallinarum (14)	1	8	16

Merck Research Laboratories, Rahway, NJ 07065, USA.

*To whom correspondence should be addressed. E-mail: hugh_rosen@merck.com